Chapter 4
Exact Solutions to the Equations of Viscous Flow

Abstract A collection of exact solutions to the equations of viscous hydrodynamics is presented, along with one for non-Newtonian flow and one which uses the Boussinesq approximation to treat a problem in natural convection.

In this chapter we present some of the very few known cases for which the equations of viscous flow can be solved without approximation. We consider only incompressible flow, since there are virtually no exact solutions known for the flow of a viscous, compressible fluid. However for a few exceptions, see Goldstein (1960), von Mises (2004) and Chap. 9 in Panton (1984).

An impressive review of exact and approximate solutions of the Navier-Stokes equation was compiled by Berker (1963).

We shall assume throughout that the body forces are zero. However the solutions are easily modified to cover the important case of a conservative body force field. For this case the covariant components of body force are derivable from a potential:

$$f_i = \frac{\partial \phi}{\partial x^i} \, .$$

Consequently, if we set

$$p^* = p - \rho\phi \, ,$$

the grouping $(\rho f_i - \partial p/\partial x^i)$ in the covariant Navier-Stokes equation (3.47) is replaced by $-\partial p^*/\partial x^i$. If the body force is gravity, we might describe this procedure as incorporating the gravitational head into the pressure head.

W.E. Langlois and M.O. Deville, *Slow Viscous Flow*,
DOI 10.1007/978-3-319-03835-3_4,

4.1 Rectilinear Flow Between Parallel Plates

In Fig. 4.1, consider that an incompressible fluid is contained in the region between two parallel infinite plates, which move steadily in their own planes. We choose a Cartesian coordinate system with x_3-axis normal to the plates and with origin midway between them, so that the plates correspond, say, to $x_3 = \pm h$. Further we let the coordinate system translate with the average velocity of the plates. Hence if the plate at $x_3 = +h$ moves with velocity components U, V in the x_1- and x_2-directions, respectively, then the plate at $x_3 = -h$ moves with velocity components $-U, -V$. Thus, the no-slip condition requires that

$$\begin{aligned} v_1 &= \pm U \quad \text{at } x_3 = \pm h \,, \\ v_2 &= \pm V \quad \text{at } x_3 = \pm h \,, \\ v_3 &= 0 \qquad \text{at } x_3 = \pm h \,. \end{aligned} \tag{4.1}$$

Since the coordinate system is not accelerated, Eqs. (2.194) and (2.195) apply. We seek a solution of the form

$$\begin{aligned} v_1 &= u(x_3) \,, \\ v_2 &= v(x_3) \,, \\ v_3 &= 0 \,, \\ p &= p(x_1) \,. \end{aligned} \tag{4.2}$$

Such a solution does, in fact, exist: the continuity equation (2.194) and the $i = 3$ component of the momentum equation (2.195) are automatically satisfied; the other two component equations reduce to

$$\mu \frac{\partial^2 u}{\partial x_3^2} = \frac{\partial p}{\partial x_1} \,, \tag{4.3}$$

$$\mu \frac{\partial^2 v}{\partial x_3^2} = 0 \,, \tag{4.4}$$

which are easily solved subject to the boundary conditions (4.1). According to (4.2), u is a function of x_3, only and p is a function of x_1 only. Consequently both sides of (4.3) are equal to the same constant, say $-G$. Thus

$$\begin{aligned} u &= U \frac{x_3}{h} + \left(\frac{G h^2}{2\mu} \right) \left(1 - \frac{x_3^2}{h^2} \right) \,, \\ v &= \frac{V x_3}{h} \,, \\ p &= C - G x_1 \,, \end{aligned} \tag{4.5}$$

where C is a constant of integration.

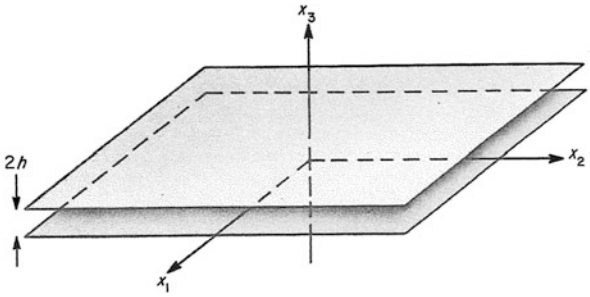

Fig. 4.1 Geometry for flow between parallel plates

A particular case corresponds to the flow between stationary plates, i.e. $U = V = 0$ in the presence of a pressure gradient. The velocity field reduces to a parabola

$$u_P = \left(\frac{Gh^2}{2\mu}\right)\left(1 - \frac{x_3^2}{h^2}\right) , \tag{4.6}$$

and this flow is know as **channel flow** or **plane Poiseuille flow** (after Jean Louis Marie Poiseuille, 1797–1869).

The **flux** Q of the flow in the x_1-direction per unit length in the x_2 direction is defined by

$$Q = \int_{-h}^{h} u \, dx_3 . \tag{4.7}$$

Integrating the first of Eqs. (4.5), we obtain

$$Q = 2G\frac{h^3}{3\mu} . \tag{4.8}$$

Thus the pressure gradient is proportional to the flux, to which the motion of the plates does not contribute.

If there is no pressure gradient, we can select an orientation of the coordinate system so that (4.5) reduces to the **Couette flow** (after Maurice Marie Alfred Couette, 1858–1943)

$$\begin{aligned} u &= U\frac{x_3}{h} , \\ v &= 0 , \\ p &= C . \end{aligned} \tag{4.9}$$

This solution is sometimes called **homogeneous shear flow**.

The general case (4.5) corresponds to Couette flow with a pressure flow superimposed; the two basic flows may be oblique to each other. Since, for the assumed form of solution (4.2), the nonlinear terms drop out of the Navier-Stokes equation, the two flows do not couple.

4.2 Plane Shear Flow of a Non-Newtonian Fluid

Let us consider the simple shear flow of the Reiner-Rivlin fluid (Eq. (2.149)) in a Cartesian orthonormal coordinate system such that

$$v_1 = \dot{\gamma}\, x_2,\ v_2 = v_3 = 0\,, \tag{4.10}$$

where $\dot{\gamma}$ is called the shear rate. The components e_{ij} of the tensor $\mathbf{e}$ vanish except for $e_{12} = e_{21} = \frac{\dot{\gamma}}{2}$, which then leads to $\mathrm{I}_2(\mathbf{e}) = -\dot{\gamma}^2/4$ and $\mathrm{I}_3(\mathbf{e}) = 0$. We will denote the matrices associated with tensors by their symbol within square brackets. Therefore the matrices $[e], [e^2]$ are given by

$$[e] = \begin{pmatrix} 0 & \frac{\dot{\gamma}}{2} & 0 \\ \frac{\dot{\gamma}}{2} & 0 & 0 \\ 0 & 0 & 0 \end{pmatrix}, \quad \left[e^2\right] = \begin{pmatrix} \frac{\dot{\gamma}^2}{4} & 0 & 0 \\ 0 & \frac{\dot{\gamma}^2}{4} & 0 \\ 0 & 0 & 0 \end{pmatrix}. \tag{4.11}$$

The corresponding stress components are then

$$T_{11} = T_{22} = -p + \varphi_2 \frac{\dot{\gamma}^2}{4}, \quad T_{33} = -p\,, \tag{4.12}$$

$$T_{12} = T_{21} = \varphi_1 \frac{\dot{\gamma}}{2} = \tau(\dot{\gamma})\,, \tag{4.13}$$

$$T_{13} = T_{23} = 0\,. \tag{4.14}$$

Let us introduce the **first normal stress differences** defined by the relations

$$N_1 = T_{11} - T_{22}, \quad N_2 = T_{22} - T_{33}\,. \tag{4.15}$$

Here we obtain

$$N_1 = 0 \quad \text{and} \quad N_2 = \varphi_2 \frac{\dot{\gamma}^2}{4}\,. \tag{4.16}$$

However, this does not correspond to the physical reality as experimental data show neither N_1 nor N_2 vanishes. We therefore need a different kind of model, namely the second-order fluid, to resolve the right normal stress differences. This model uses Rivlin-Ericksen tensors, a concept described in Deville and Gatski (2012). It can be

shown that all three functions N_1, N_2, τ depend on the nature of the fluid, and are called the **viscometric functions** of the material. Note also that in the Newtonian case $N_2 = 0$, indicating that for this kind of fluid, there is no imbalance in the first normal stress differences.

4.3 The Flow Generated by an Oscillating Plate

Let us now suppose that an infinite flat plate at the bottom of an infinitely deep sea of fluid executes linear harmonic motion parallel to itself. We let the plate lie in the $x_3 = 0$ plane of a Cartesian coordinate system, so oriented that the oscillation is along the x_1-axis. The location of the origin is unimportant, but the x_i-system is fixed in space, not in the oscillating plate. The motion of the plate generates in the fluid a rectilinear flow, partially in-phase, partially out-of-phase, with the plate. The pressure, however, remains constant.

If the velocity-amplitude and frequency of the plate motion are denoted, respectively, by A and ω, the no-slip condition requires that

$$v_1 = = A\cos\omega t \quad \text{at } x_3 = 0\,, \tag{4.17}$$

$$v_2 = v_3 = 0 \quad \text{at } x_3 = 0\,. \tag{4.18}$$

If we set

$$\begin{aligned} v_1 &= f(x_3)\cos\omega t + g(x_3)\sin\omega t\,,\\ v_2 &= v_3 = 0\,,\\ p &= constant\,, \end{aligned} \tag{4.19}$$

the equations of motion (2.194), (2.195) are satisfied, provided only that

$$(\omega g - \nu f'')\cos\omega t = (\omega f + \nu g'')\sin\omega t\,. \tag{4.20}$$

Equation (4.20) can hold for all values of t only if both sides vanish independently. Thus

$$\begin{aligned} \omega g - \nu f'' &= 0\,,\\ \omega f + \nu g'' &= 0\,. \end{aligned} \tag{4.21}$$

It is readily verified that the general solution of this system is

$$\begin{aligned} f(x_3) &= e^{-kx_3}(c_1\cos kx_3 + c_2\sin kx_3) + e^{+kx_3}(c_3\cos kx_3 + c_4\sin kx_3)\,,\\ g(x_3) &= e^{-kx_3}(c_1\sin kx_3 - c_2\cos kx_3) - e^{+kx_3}(c_3\sin kx_3 - c_4\cos kx_3)\,, \end{aligned} \tag{4.22}$$

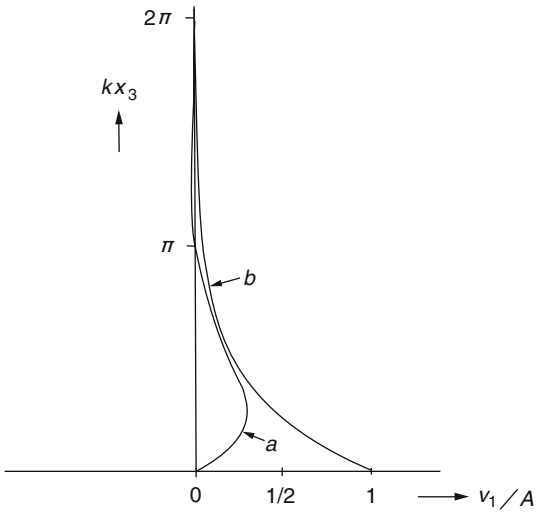

Fig. 4.2 Velocity distribution above an oscillating plate. (*a*) Plate at maximum displacement. (*b*) Plate at midcycle

where

$$k = \sqrt{\frac{\omega}{2\nu}} \,. \tag{4.23}$$

Since the growing exponentials are not physically admissible, we set

$$c_3 = c_4 = 0 \,. \tag{4.24}$$

The remaining constants are evaluated from the boundary condition (4.17):

$$c_1 = A,\ c_2 = 0 \,. \tag{4.25}$$

We then have

$$\begin{aligned} v_1 &= Ae^{-kx_3}(\cos kx_3 \cos \omega t + \sin kx_3 \sin \omega t) \\ &= Ae^{-kx_3} \cos(\omega t - kx_3) \,. \end{aligned} \tag{4.26}$$

Thus the oscillating plate sets up a corresponding oscillation in the fluid. As we move away from the plate, the amplitude decays exponentially and the phase lag with respect to the plate motion varies linearly. Two fluid layers a distance $2\pi/k$ apart oscillate in phase. This distance, which, by (4.23), is equal to $2\pi\sqrt{2\nu/\omega}$, is called the **depth of penetration** of the harmonic motion. That it increases with viscosity and decreases with frequency is not surprising: if we slowly oscillate a flat plate in a sticky fluid, we expect to drag large masses of fluid along with the plate;

on the other hand, if we move the plate rapidly in a fluid of low viscosity, we expect the fluid essentially to ignore the plate, except in a thin boundary-layer.

The velocity profile above an oscillating plate is illustrated in Fig. 4.2.

4.4 Transient Flow in a Semi-infinite Space

Let us consider the case in which the plate executes a motion more general than steady-state oscillation. To make it definite, let us suppose that the plate, and the fluid above it, are at rest until time zero, when the plate begins to move in the x_1-direction[1] with velocity $V(t)$. If we set

$$\begin{aligned} v_1 &= v(x_3, t) \,, \\ v_2 &= v_3 = 0 \,, \\ p &= \text{constant} \,, \end{aligned} \tag{4.27}$$

the equations of motion (2.194), (2.195) are satisfied if

$$\frac{\partial v}{\partial t} = \nu \frac{\partial^2 v}{\partial x_3^2} \,. \tag{4.28}$$

Thus the velocity generated by the moving plate diffuses through the fluid according to the heat equation. This equation can be solved subject to the initial condition

$$v(x_3, 0) = 0 \,, \tag{4.29}$$

and to the boundary condition

$$v(0, t) = V(t) \,, \tag{4.30}$$

by straightforward application of the Laplace transform. Some instructive cases are worked out in Schlichting (1960); unsteady motion between parallel plates is also considered. The reader is also referred to Dowty (1963).

If we assume $V(t) = V$, with V a constant, then we can work out easily a closed form solution. The initial and boundary conditions are recapitulated as

$$t < 0, \quad v = 0, \quad \forall\ x_3 \,, \tag{4.31}$$

$$t \geqslant 0, \quad v = V, \quad \text{at } x_3 = 0 \,, \tag{4.32}$$

$$v = 0, \quad \text{at } x_3 = \infty \,. \tag{4.33}$$

[1] Motion in the x_2-direction could be superimposed; the resulting fluid motions do not couple.

Equation (4.28) is a diffusion type equation similar to the heat equation. We will transform this partial differential equation into an ordinary differential equation by a change of variables that is based on similarity considerations. As the problem has no other space variable than x_3 and no other time scale than t, one combines them to form the dimensionless group

$$\eta = \frac{x_3}{2\sqrt{\nu t}} . \tag{4.34}$$

This change of variable will produce an ordinary differential equation whose solution is a function of η. This solution is called a **self-similar solution** as the velocity profile with respect to x_3 is similar at any time t. Setting

$$v = V\, f(\eta) , \tag{4.35}$$

Eq. (4.28) becomes

$$f'' + 2\eta f' = 0 , \tag{4.36}$$

with the conditions

$$\eta = 0,\ f = 1; \quad \eta = \infty, f = 0 . \tag{4.37}$$

Integrating (4.36), one obtains

$$f = A \int_0^{\eta} e^{-\eta'^2} d\eta' + B . \tag{4.38}$$

With the conditions (4.37), one gets for $\eta = 0$, $B = 1$ and for $\eta = \infty$, $A = -2/\sqrt{\pi}$. In terms of the error function erf(x) defined by

$$\text{erf}\,(x) = \frac{2}{\sqrt{\pi}} \int_0^x e^{-\tau^2} d\tau , \tag{4.39}$$

which makes erf$(\infty) = 1$, Eq. (4.38) becomes

$$f = 1 - \text{erf}\,\eta . \tag{4.40}$$

The velocity profile for $t > 0$ is

$$v = V \left[1 - \text{erf}(\frac{x_3}{2\sqrt{\nu t}}) \right] . \tag{4.41}$$

and is shown in Fig. 4.3.

The penetration depth of the plate movement in the semi-infinite space is related to the question: for t fixed, what is the distance to the plate where the velocity

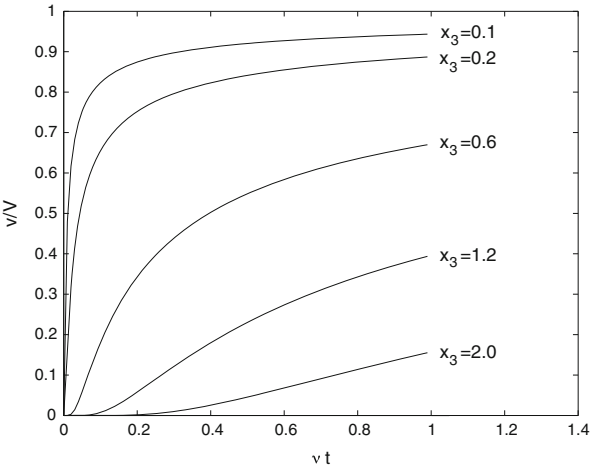

Fig. 4.3 Transient flow in a semi-infinite space

reaches, for example, 1 % of the V value? From numerical erf values, the function $1 - \text{erf}(\eta)$ is 0.01 for $\eta \sim 2$. The penetration depth δ is consequently given by

$$\eta_\delta = \frac{\delta}{2\sqrt{\nu t}} \simeq 2, \quad \delta \simeq 4\sqrt{\nu t}\ . \tag{4.42}$$

It is proportional to the square root of the kinematic viscosity and time. If the viscosity is very small, the fluid "sticks" less to the wall and the effect of the wall presence is reduced. If t goes to infinity, the velocity at each position in the semi-infinite space goes to V.

4.5 Channel Flow with a Pulsatile Pressure Gradient

Blood flow in the vascular tree is driven by the pulsating pressure gradient produced by the heart that is acting as a pump. In order to avoid (temporarily) the geometrical complexity of cylindrical coordinates appropriate for blood flow in the arteries, we will tackle a simplified version of the problem, namely the plane channel flow under an oscillating pressure gradient.

Recall that the standard Poiseuille flow with a steady constant pressure gradient denoted by G gives rise to the parabolic velocity profile (4.6). Let us add now an oscillating component characterized by the pulsation ω such that

$$-\frac{1}{\rho}\frac{\partial p}{\partial x_1} = -G - C\cos\omega t\ , \tag{4.43}$$

with C a constant obtained from experimental data, for example. For the sake of simplicity in the analytical treatment, it is customary to resort to Fourier

representation and use the following relation

$$-\frac{1}{\rho}\frac{\partial p}{\partial x_1} = -G - \Re(Ce^{i\omega t}) \,, \tag{4.44}$$

where $\Re$ means the real part. As a steady state oscillating solution is sought for the velocity field, the solution is written as a complex function

$$v_1 = u_P + \Re\left(u(\omega, x_3)e^{i\omega t}\right) \,, \tag{4.45}$$

where the Poiseuille solution u_P given by Eq. (4.6) corresponds to constant pressure gradient.

The Navier-Stokes equations lead to the relation

$$\frac{\partial v_1}{\partial t} = -\frac{1}{\rho}\frac{\partial p}{\partial x_1} + \nu\frac{\partial^2 v_1}{\partial x_3^2} \,. \tag{4.46}$$

With Eqs. (4.44) and (4.45), Eq. (4.46) gives

$$i\,\omega\, u = -C + \nu\frac{\partial^2 u}{\partial x_3^2} \,. \tag{4.47}$$

The boundary conditions are

$$u(h) = 0, \quad \frac{\partial u}{\partial x_3}(0) = 0 \,. \tag{4.48}$$

The solution of (4.47) is

$$u = \Re\left[\frac{iC}{\omega}\left(1 - \frac{\cosh\sqrt{\frac{i\omega}{\nu}}x_3}{\cosh\sqrt{\frac{i\omega}{\nu}}h}\right)\right] \,. \tag{4.49}$$

Taking the relation $i^{1/2} = (1+i)/\sqrt{2}$ into account, the real part of (4.49) yields the velocity field

$$v_1 = u_P - \frac{C}{\omega}\left[\left(1 - \frac{f_1(\omega, x_3)}{f_3(kh)}\right)\sin\omega t - \frac{f_2(\omega, x_3)}{f_3(kh)}\cos\omega t\right] \,, \tag{4.50}$$

where the various notations are defined as follows

$$\begin{aligned} k &= \sqrt{\frac{\omega}{2\nu}} \,, \\ cc(x) &= \cos(x)\cosh(x) \,, \\ ss(x) &= \sin(x)\sinh(x) \,, \end{aligned}$$

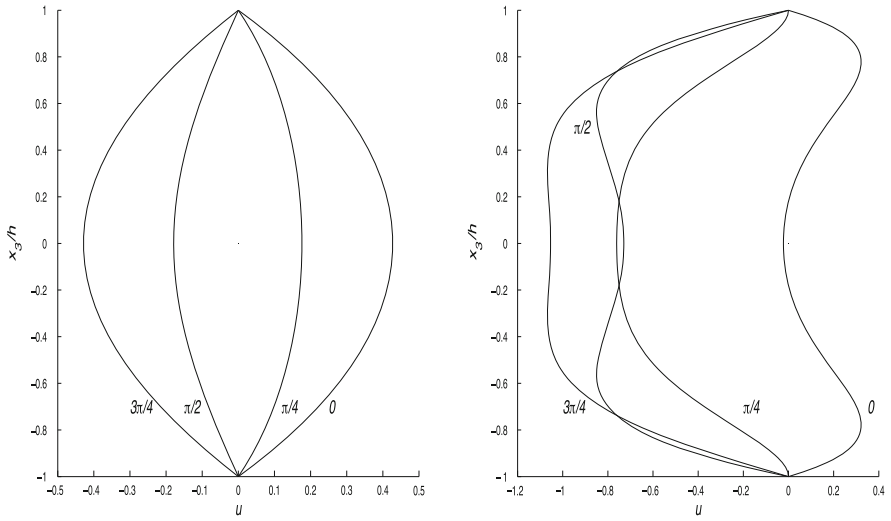

Fig. 4.4 Pulsating velocity field with $\omega = 1$; *left*: $k = 1/\sqrt{2}$; *right*: $k = 5/\sqrt{2}$

$$
\begin{aligned}
f_1(\omega, x_3) &= cc(kx_3)cc(kh) + ss(kx_3)ss(kh) \,, \\
f_2(\omega, x_3) &= cc(kx_3)ss(kh) - ss(kx_3)cc(kh) \,, \\
f_3(\omega) &= cc^2(\omega) + ss^2(\omega) \,.
\end{aligned}
\tag{4.51}
$$

Figure 4.4 shows the time evolution of the velocity profile for two different values of k. The left part represents the flow for a low frequency case or when the viscous forces are important, i.e. $hk \ll 1$, whereas the right part corresponds to high frequency forcing or to a fluid with low viscosity. The low frequency solution may be obtained by taking the limit of Eq. (4.50) when $k \to 0$. Since $cc(x) \to 1$ and $ss(x)$ is asymptotic to x^2 as $x \to 0$, one has

$$
v_1 = u_P + \frac{Ch^2}{2\nu} \cos \omega t \left(1 - (\frac{x_3}{h})^2\right) \,, \tag{4.52}
$$

so that the pulsating term is still a parabola with a modified amplitude which is given by the oscillating part of the pressure gradient in (4.43). The high frequency case or the equivalent inviscid fluid may be treated with the approximation $hk \gg 1$. Then, since $cc(x)$ and $ss(x)$ are asymptotic, respectively, to $1/2\, e^x \cos x$ and $1/2\, e^x \sin(x)$ as $x \to \infty$, the limit solution reads

$$
v_1 = u_P - \frac{C}{\omega} \left(\sin \omega t - \sin(\omega t - \eta) e^{-\eta}\right) \,, \tag{4.53}
$$

where the new variable η measuring the distance from the upper wall is defined as

$$\eta = k(h - x_3) = \frac{h - x_3}{\sqrt{2\nu/\omega}} \,. \tag{4.54}$$

Note that the first term of the oscillating part of (4.53) is the response of the inviscid fluid ($\nu = 0$) to the pressure gradient. As soon as we are inside the fluid the second oscillating term goes to zero leaving the flow oscillating under the influence of the pressure gradient.

4.6 Poiseuille Flow

Probably the most important exact solution in applied viscous hydrodynamics is the Poiseuille solution for pressure flow through a straight circular pipe of uniform diameter. Let a cylindrical polar coordinate system be defined with z-axis along the axis of the pipe; in view of the axial symmetry of the situation, the specific orientation of the $\theta = 0$ direction is unimportant. If the radius of the pipe is denoted by R, the no-slip condition requires

$$v_r = v_\theta = v_z = 0 \quad \text{at } r = R \,. \tag{4.55}$$

We seek a solution to Eqs. (3.77) through (3.80) in the form

$$\begin{aligned} v_r &= v_\theta = 0 \,, \\ v_z &= u(r) \,, \\ p &= p(z) \,. \end{aligned} \tag{4.56}$$

The continuity equation (3.77) is automatically satisfied, as are the momentum equations (3.78) and (3.79). There remains only (3.80), which reduces to

$$\mu \left(\frac{\partial^2 u}{\partial r^2} + \frac{1}{r} \frac{\partial u}{\partial r} \right) = \frac{\partial p}{\partial z} \,. \tag{4.57}$$

As for the flow between plates, both sides must be equal to the same constant, say $-G$. With the boundary conditions (4.55) and the restriction that the velocity be finite at the tube axis,

$$u = \left(\frac{GR^2}{4\mu} \right) \left(1 - \frac{r^2}{R^2} \right) \,, \tag{4.58}$$

$$p = C - Gz \,, \tag{4.59}$$

where C is a constant of integration.

If we denote by Q the volume rate of flow through the pipe, so that

$$Q = 2\pi \int_0^R ru\, dr\,, \tag{4.60}$$

integration of (4.58) yields

$$Q = \pi \frac{GR^4}{8\mu}\,. \tag{4.61}$$

We can superimpose a swirl without disturbing the parabolic velocity profile (4.58). Let us suppose that we rotate the pipe about its own axis, not necessarily with constant angular velocity. The boundary conditions (4.55) must then be modified:

$$v_r = v_z = 0 \quad \text{at } r = R\,, \tag{4.62}$$

$$v_\theta = R\omega(t) \quad \text{at } r = R. \tag{4.63}$$

If we set

$$\begin{aligned} v_r &= 0, \\ v_\theta &= v(r,t)\,, \\ v_z &= u(r)\,, \end{aligned} \tag{4.64}$$

where $u(r)$ is the Poiseuille solution (4.58), the continuity equation (3.77) is automatically satisfied.

The pressure field (4.59) will not quite suffice. As evidenced by Eq. (3.78), an r-dependence must be added to balance the centrifugal force generated by v_θ. We set

$$p(z,r,t) = C - Gz + \rho \int_0^r r^{-1}[v(r,t)]^2 dr\,. \tag{4.65}$$

With (4.64) and (4.65), Eqs. (3.78) and (3.80) are satisfied. There remains only (3.79), which reduces to

$$\frac{\partial v}{\partial t} = \nu \left(\frac{\partial^2 v}{\partial r^2} + \frac{1}{r}\frac{\partial v}{\partial r} - \frac{v}{r^2} \right)\,. \tag{4.66}$$

By way of example, suppose that the pipe wall undergoes steady-state torsional oscillation, so that

$$\omega(t) = A \cos nt\,. \tag{4.67}$$

We expect that the resulting swirl will have an in-phase and an out-of-phase component, so that

$$v(r,t) = f(r)\cos nt + g(r)\sin nt\,. \tag{4.68}$$

Substituting into (4.66),

$$(\cos nt)\left(\frac{ng}{\nu} - f'' - \frac{f'}{r} + \frac{f}{r^2}\right) = (\sin nt)\left(\frac{nf}{\nu} + g'' + \frac{g'}{r} - \frac{g}{r^2}\right) . \tag{4.69}$$

If (4.69) is to hold for all values of t, both sides must vanish independently. Thus

$$\frac{ng}{\nu} - f'' - \frac{f'}{r} + \frac{f}{r^2} = 0 , \tag{4.70}$$

$$\frac{nf}{\nu} + g'' + \frac{g'}{r} - \frac{g}{r^2} = 0 . \tag{4.71}$$

If we multiply (4.70) by i and subtract from (4.71), we obtain

$$\frac{n}{\nu}(f - ig) + \left(\frac{d^2}{dr^2} + \frac{1}{r}\frac{d}{dr} - \frac{1}{r^2}\right)(g + if) = 0 . \tag{4.72}$$

By setting

$$F(r) = f(r) - ig(r) , \tag{4.73}$$

(4.72) can be written as Bessel's equation of order unity:

$$\frac{d^2F}{dr^2} + \frac{1}{r}\frac{dF}{dr} + \left(\frac{i^3 n}{\nu} - \frac{1}{r^2}\right) F = 0 . \tag{4.74}$$

Since $F(0)$ must be finite, we reject the Neumann function as an admissible solution. Therefore

$$F(r) = cJ_1(i^{3/2} r\sqrt{n/\nu}) , \tag{4.75}$$

where c is a (complex) constant of integration. Comparing (4.63), (4.64), (4.67), (4.68), (4.73), we see that

$$F(R) = RA , \tag{4.76}$$

so that

$$c = \frac{\operatorname{ber}_1 R\sqrt{n/\nu} - i \operatorname{bei}_1 R\sqrt{n/\nu}}{(\operatorname{ber}_1 R\sqrt{n/\nu})^2 + (\operatorname{bei}_1 R\sqrt{n/\nu})^2} RA , \tag{4.77}$$

where $\operatorname{ber}_1 z$ and $\operatorname{bei}_1 z$ denote, respectively, the real and imaginary parts of $J_1(i^{3/2}z)$. With (4.73) and (4.75), we then obtain

$$f(r) = \frac{RA}{(\mathrm{ber}_1 R\sqrt{n/\nu})^2 + (\mathrm{bei}_1 R\sqrt{n/\nu})^2}(\mathrm{ber}_1 R\sqrt{n/\nu}\,\mathrm{ber}_1 r\sqrt{n/\nu} + \mathrm{bei}_1 R\sqrt{n/\nu}\,\mathrm{bei}_1 r\sqrt{n/\nu}) ,$$

$$g(r) = \frac{RA}{(\mathrm{ber}_1 R\sqrt{n/\nu})^2 + (\mathrm{bei}_1 R\sqrt{n/\nu})^2}(\mathrm{bei}_1 R\sqrt{n/\nu}\,\mathrm{ber}_1 r\sqrt{n/\nu} - \mathrm{ber}_1 R\sqrt{n/\nu}\,\mathrm{bei}_1 r\sqrt{n/\nu}) . \quad (4.78)$$

The remarks in Sect. 4.3 concerning the penetration of the boundary motion into the fluid carry over *mutatis mutandis* to the torsional oscillation of a circular pipe. Also in analogy with Sect. 4.3, more general rotary motion of the pipe can be treated by applying the Laplace transform to Eq. (4.66). Unsteady longitudinal motion of the pipe can also be treated.

In the next chapter we shall consider the exact solution of the problem of steady-state flow through a pipe of non-circular cross section.

4.7 Starting Transient Poiseuille Flow

We will examine the transient flow in a circular pipe where the fluid starts from rest to reach the Poiseuille steady parabolic profile (4.58). The only non vanishing velocity component is v_z and the pressure gradient goes instantaneously at $t = 0$ from zero to the value $-G$ everywhere. The dynamic equation is from (3.80)

$$G + \mu\left(\frac{\partial^2 v_z}{\partial r^2} + \frac{1}{r}\frac{\partial v_z}{\partial r}\right) = \rho\frac{\partial v_z}{\partial t} , \quad (4.79)$$

with the initial condition

$$v_z(r, 0) = 0, \quad 0 \le r \le R , \quad (4.80)$$

and the boundary condition

$$v_z(R, t) = 0, \forall t . \quad (4.81)$$

In order to render (4.79) homogeneous, let us change variables

$$w(r, t) = \frac{G}{4\mu}\left(R^2 - r^2\right) - v_z(r, t) . \quad (4.82)$$

The new variable will be solution of the equation

$$\frac{\partial^2 w}{\partial r^2} + \frac{1}{r}\frac{\partial w}{\partial r} = \frac{1}{\nu}\frac{\partial w}{\partial t} , \quad (4.83)$$

with the initial condition

$$w(r,0) = \frac{G}{4\mu}\left(R^2 - r^2\right), \tag{4.84}$$

and the boundary condition

$$w(R,t) = 0, \quad \forall t\ . \tag{4.85}$$

Through the transient phase, the velocity v_z will increase till the steady state (4.58) is reached, whereas the transient perturbation $w(r,t)$ will decay to zero. To solve (4.83), we proceed by separation of variables

$$w(r,t) = f(r)g(t)\ . \tag{4.86}$$

Substituting in (4.83), one gets

$$\frac{dg(t)}{dt} + C\nu\, g(t) = 0\,, \tag{4.87}$$

$$\frac{d^2 f}{dr^2} + \frac{1}{r}\frac{df}{dr} + C\ f = 0\,, \tag{4.88}$$

where C is an arbitrary constant. The solution of (4.87) reads

$$g(t) = B\exp(-C\nu t)\ . \tag{4.89}$$

As $w(r,t)$ decreases with respect to time, we assume that C will involve only positive values so that C can be written λ^2/R^2. This will ease the next computations, as we will observe. Equation (4.88) then becomes

$$\frac{d^2 f}{dr^2} + \frac{1}{r}\frac{df}{dr} + \frac{\lambda^2}{R^2}\ f = 0\,. \tag{4.90}$$

The change of variable $\lambda r/R = z$ leads (4.90) to the canonical form of the Bessel equation

$$\frac{d^2 f}{dz^2} + \frac{1}{z}\frac{df}{dz} + (1 - \frac{k^2}{z^2})\ f = 0\,, \tag{4.91}$$

whose general solution is given by

$$f = C_1 J_k(z) + C_2 Y_k(z)\,, \tag{4.92}$$

where the functions J_k and Y_k are Bessel functions of first and second kind, respectively, of order k and C_1, C_2 are arbitrary constants. Consequently, the solution of (4.90) is

$$f = C_1 J_0(\frac{\lambda r}{R}) + C_2 Y_0(\frac{\lambda r}{R}) . \tag{4.93}$$

As Y_0 goes to $-\infty$ when $r \to 0$, one concludes that $C_2 = 0$ for w to remain finite on the axis. The general solution of (4.83) becomes

$$w(r,t) = C_3 J_0(\frac{\lambda r}{R}) \exp(-\frac{\lambda^2}{R^2}\nu t) . \tag{4.94}$$

The solution (4.94) verifies condition (4.85) for λ values, denoted λ_n, given by the zeroes of the Bessel function J_0

$$J_0(\lambda_n) = 0 . \tag{4.95}$$

The solution is obtained as

$$w(r,t) = \frac{G}{4\mu} \sum_{n=1}^{\infty} c_n \, J_0(\frac{\lambda_n r}{R}) \exp(-\frac{\lambda_n^2}{R^2}\nu t), \tag{4.96}$$

and the coefficients c_n are determined by (4.84):

$$R^2 - r^2 = \sum_{n=1}^{\infty} c_n \, J_0(\frac{\lambda_n r}{R}) . \tag{4.97}$$

To solve Eq. (4.97), let us recall the orthogonality properties of Bessel functions as expressed by Lommel integrals

$$\int_0^1 z \, J_n(\lambda_i z) J_n(\lambda_j z) dz = 0, \quad \lambda_i \neq \lambda_j , \tag{4.98}$$

$$\int_0^1 z \, J_n^2(\lambda_i z) dz = \frac{1}{2}[J_n'(\lambda_i)]^2 . \tag{4.99}$$

Solution of (4.97) is obtained with $z = r/R$ as

$$c_n = \frac{2R^2}{[J_0'(\lambda_n)]^2} \int_0^1 (1 - z^2) z \, J_0(\lambda_n z) dz . \tag{4.100}$$

The evaluation of the two integrals in (4.100) is carried out using successively the recurrence relationships (4.102) and then (4.101) Abramowitz and Stegun (1972) with $\ell = 2, m = 0$

$$\int z^{\ell+1} J_m(z)dz = z^{\ell+1} J_{m+1}(z) + (\ell - m) z^{\ell} J_m(z) - (\ell^2 - m^2) \int z^{\ell-1} J_m(z)dz \,, \tag{4.101}$$

$$\int_{z_0}^{z} z^m J_{m-1}(z)dz = [z^m J_m(z)]_{z_0}^{z} \,, \tag{4.102}$$

$$z J'_m(z) = m J_m(z) - z J_{m+1}(z) \,. \tag{4.103}$$

This yields

$$\int_0^1 z\, J_0(\lambda_n z)dz = \frac{1}{\lambda_n} J_1(\lambda_n) \,, \tag{4.104}$$

$$\int_0^1 z^3\, J_0(\lambda_n z)dz = \frac{1}{\lambda_n^4} \left[\lambda_n^3 J_1(\lambda_n) + 2\lambda_n^2 J_0(\lambda_n) - 4\lambda_n J_1(\lambda_n)\right] \,, \tag{4.105}$$

$$= \frac{1}{\lambda_n} J_1(\lambda_n) - \frac{4}{\lambda_n^3} J_1(\lambda_n) \,.$$

One finds with the help of the relation $[J'_0(\lambda_n)]^2 = [J_1(\lambda_n)]^2$:

$$c_n = \frac{8R^2}{\lambda_n^3 J_1(\lambda_n)} \,. \tag{4.106}$$

Taking Eqs. (4.82), (4.96) and (4.106) into account, the velocity profile is

$$v_z(r,t) = \frac{G}{4\mu}\left(R^2 - r^2\right) - \frac{2GR^2}{\mu} \sum_{n=1}^{\infty} \frac{J_0(\frac{\lambda_n r}{R})}{\lambda_n^3 J_1(\lambda_n)} \exp(-\frac{\lambda_n^2}{R^2} \nu t) \,. \tag{4.107}$$

Figure 4.5 shows the velocity variation with respect to time.

4.8 Pulsating Flow in a Circular Pipe

We come back to the blood flow in arteries. Assuming that arteries are rigid circular pipes, —an assumption far from the physiological phenomena as arterial walls deform and move under pressure waves Zamir (2000)—, we are faced with a time-periodic pressure gradient driving the Poiseuille flow. The cardiac cycle is indeed time-periodic and therefore the pressure gradient should be represented by a Fourier series. For the sake of simplicity we will consider only a Fourier in such a way that

$$\frac{\partial p}{\partial z} = -Ce^{i\omega t} \,, \tag{4.108}$$

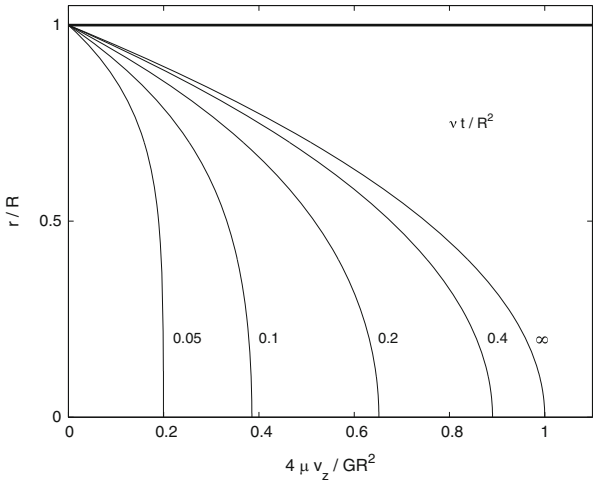

Fig. 4.5 Transient Poiseuille flow in a circular pipe

with ω the angular frequency. The flow governing equation is obtained from (3.80):

$$Ce^{i\omega t} + \mu\left(\frac{\partial^2 v_z}{\partial r^2} + \frac{1}{r}\frac{\partial v_z}{\partial r}\right) = \rho\frac{\partial v_z}{\partial t}\,, \tag{4.109}$$

and a solution is sought in terms of the Fourier representation

$$v_z = u(r)e^{i\omega t}\,. \tag{4.110}$$

The combination of Eqs. (4.109) and (4.110) generates the solution

$$u = \frac{C}{i\rho\omega}\left(1 - \frac{J_0(i^{3/2}\alpha r/R)}{J_0(i^{3/2}\alpha)}\right)\,, \tag{4.111}$$

in which there appears a dimensionless number α called the **Womersley number** defined as

$$\alpha = R\sqrt{\frac{\omega}{\nu}}\,. \tag{4.112}$$

Note that the Womersley number is the square root of the oscillatory Reynolds number (2.241).

The solution (4.111) was obtained with the boundary conditions

$$u(R) = 0, \quad \frac{du}{dr}(r = 0) = 0\,. \tag{4.113}$$

The function $J_0(i^{3/2}\sqrt{\frac{\omega}{\nu}}r) = J_0(i^{3/2}\alpha r/R)$ is the Kelvin function of order 0.

As the Womersley number is the ratio of the radius to the penetration depth, it is a characteristic feature of pulsatile blood flow. Typical values of α in the aorta range from 20 for a human in good health to 8 for a cat. Another way of interpreting the Womersley number consists in estimating the distance from the rigid wall, say δ, where the viscous forces and the inertia are of equal magnitude. Near the wall, viscosity is dominant and a rough estimate of the viscous forces is $\mu U/\delta^2$. Near the symmetry axis, inertia dominates and yields the estimate $\rho\omega U$. Equating the two forces leads to the definition

$$\delta = \frac{\nu}{\omega} . \tag{4.114}$$

If α is large, the viscous effects are confined to a region very close to the wall. In the centre of the flow, the dynamics will be driven by the equilibrium of inertia and pressure forces, resulting in a velocity profile that will be more blunt than the parabolic profile that comes from the balance of viscous and pressure forces.

4.9 Helical Flow in an Annular Region

4.9.1 The Newtonian Case

In this section we treat the motion of fluid contained between two concentric circular pipes of constant radii R_1 and R_2 with, say, $R_1 < R_2$ as indicated in Fig. 4.6. The pipes rotate about their common axis with constant angular velocities ω_1 and ω_2, respectively. In addition the pipes may translate steadily, parallel to their common axis; let us say that the outer pipe translates with velocity U relative to the inner.

We define a cylindrical coordinate system r, θ, z which translates with the inner pipe but does not rotate with it. The z-axis lies along the common axis of the pipes; because of the axial symmetry, the orientation of the $\theta = 0$ axis is unimportant.

Since the cylindrical coordinate system is not accelerated, the fluid motion is governed by Eqs. (3.77) through (3.80). The no-slip condition requires that

$$\begin{aligned} &v_r = v_z = 0, \quad v_\theta = R_1\omega_1 \quad \text{at } r = R_1 ; \\ &v_r = 0, \quad v_\theta = R_2\omega_2, \quad v_z = U \quad \text{at } r = R_2 . \end{aligned} \tag{4.115}$$

From our experiences with the exact solutions found in previous sections, we expect that

$$\begin{aligned} v_r &= 0 , \\ v_\theta &= v(r) , \\ v_z &= u(r) , \\ p &= C - Gz + \rho \int_0^r r^{-1}[v(r)]^2 dr . \end{aligned} \tag{4.116}$$

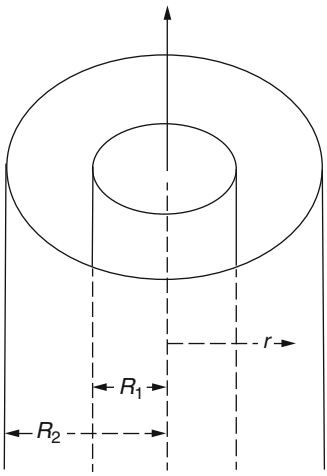

Fig. 4.6 Helical flow geometry

The continuity equation is indeed satisfied, as is Eq. (3.78). Equation (3.79) reduces to

$$\frac{d^2v}{dr^2} + \frac{1}{r}\frac{dv}{dr} - \frac{v}{r^2} = 0\,, \tag{4.117}$$

and Eq. (3.80) becomes

$$\frac{d^2u}{dr^2} + \frac{1}{r}\frac{du}{dr} = -\frac{G}{\mu}\,. \tag{4.118}$$

Thus the rotary flow and the axial flow do not couple. Integrating (4.117) subject to the boundary conditions on v_θ yields the **axisymmetric Couette flow**

$$v = \left(\frac{R_2^2\omega_2 - R_1^2\omega_1}{R_2^2 - R_1^2}\right) r + \left(\frac{\omega_1 - \omega_2}{R_2^2 - R_1^2}\right)\frac{R_1^2 R_2^2}{r}\,. \tag{4.119}$$

Integrating (4.118) subject to the boundary conditions on v_r yields

$$u = \frac{G}{4\mu}\left[R_1^2 - r^2 + \frac{(R_2^2 - R_1^2)\ln(r/R_1)}{\ln(R_2/R_1)}\right] + U\frac{\ln(r/R_1)}{\ln(R_2/R_1)}\,. \tag{4.120}$$

If the pipes do not translate relative to one another, so that $U = 0$, Eq. (4.120) describes **pressure flow in a coaxial pipe**. The opposite case, for which $G = 0$ but $U \neq 0$, is referred to as **drag flow**, but the term is not in common use. The general case described by (4.119) and (4.120) might be termed pressure flow with superimposed Couette flow and drag flow.

As in Poiseuille's problem, the exact solution presented here can be generalized by permitting unsteady motion of the pipes parallel to themselves.

4.9.2 The Non-Newtonian Circular Couette Flow

Circular Couette flow occurs in the gap between two rotating concentric cylinders. The inner cylinder of radius R_1 has the angular velocity ω_1 while the outer cylinder of radius R_2 spins at ω_2. The apparatus has a height H which is much larger than the radius of either cylinder so that the apparatus height is supposed infinite. Referring to the previous cylindrical coordinates system r, θ, z, the steady state velocity field is such that

$$v_r = 0, \quad v_\theta = v_\theta(r), \quad v_z = 0\,. \tag{4.121}$$

This v_θ velocity field is then determined from the integration of the θ-momentum equation

$$\begin{aligned}\rho\Big(\frac{\partial v_\theta}{\partial t} + v_r\frac{\partial v_\theta}{\partial r} + \frac{v_\theta}{r}\frac{\partial v_\theta}{\partial \theta} + v_z\frac{\partial v_\theta}{\partial z} + \frac{v_r v_\theta}{r}\Big)\\ = \frac{\partial T_{r\theta}}{\partial r} + \frac{1}{r}\frac{\partial T_{\theta\theta}}{\partial \theta} + \frac{\partial T_{\theta z}}{\partial z} + \frac{2T_{r\theta}}{r}\,,\end{aligned} \tag{4.122}$$

which reduces to

$$\frac{1}{r^2}\frac{d}{dr}\left(r^2\, T_{r\theta}\right) = 0\,. \tag{4.123}$$

The stress component $T_{r\theta}$ of (2.149) is given by the relation

$$T_{r\theta} = \frac{\varphi_1}{2}\left(\frac{\partial v_\theta}{\partial r} - \frac{v_\theta}{r}\right)\,. \tag{4.124}$$

Taking (4.124) into account, the integration of (4.123) with the boundary conditions $v_\theta(R_1) = R_1\omega_1$ and $v_\theta(R_2) = R_2\omega_2$ yields the velocity field (4.119).

In the case of a fixed outer cylinder $\omega_2 = 0$ and the velocity is given by

$$v_\theta = Ar + \frac{B}{r} = \frac{\omega_1 R_1^2}{R_2^2 - R_1^2}\left(\frac{R_2^2}{r} - r\right)\,. \tag{4.125}$$

The r-momentum equation

$$\begin{aligned}\rho\Big(\frac{\partial v_r}{\partial t} + v_r\frac{\partial v_r}{\partial r} + \frac{v_\theta}{r}\frac{\partial v_r}{\partial \theta} + v_z\frac{\partial v_r}{\partial z} - \frac{v_\theta^2}{r}\Big)\\ = \frac{\partial T_{rr}}{\partial r} + \frac{1}{r}\frac{\partial T_{r\theta}}{\partial \theta} + \frac{\partial T_{rz}}{\partial z} + \frac{T_{rr} - T_{\theta\theta}}{r}\end{aligned}$$

simplifies and gives

$$\frac{d\,T_{rr}}{dr} + \frac{1}{r}\,(T_{rr} - T_{\theta\theta}) = -\rho\frac{v_\theta^2}{r}\,. \tag{4.126}$$

With the stress component

$$T_{rr} = -p + \frac{\varphi_2}{4}\left(\frac{\partial v_\theta}{\partial r} - \frac{v_\theta}{r}\right)^2,$$

Eq. (4.126) yields

$$-\frac{\partial p}{\partial r} + \varphi_2\frac{\partial}{\partial r}\left(\frac{B^2}{r^4}\right) = -\rho\frac{v_\theta^2}{r}\,. \tag{4.127}$$

As $T_{zz} = -p$, one obtains

$$-T_{zz} = p = \varphi_2\,\frac{B^2}{r^4}\,|_{R_1}^{r} + \int_{R_1}^{r}\rho\frac{v_\theta^2}{r}\,dr + C \tag{4.128}$$

$$= p(R_1) + \varphi_2\,\frac{B^2}{r^4} + \int_{R_1}^{r}\rho\frac{v_\theta^2}{r}\,dr\,. \tag{4.129}$$

If the fluid is Newtonian, $\varphi_2 = 0$ and the pressure increases from the inner to the outer cylinder. The fluid rises along the outer cylinder under centrifugal forces. For the non-Newtonian fluid, if $\varphi_2 > 0$ and if B is sufficiently large under a high shear due to a small gap between the cylinders, the pressure increases when one approaches the inner cylinder and this produces the rod-climbing effect as shown in Fig. 2.5.

4.10 Hamel's Problem: Flow in a Wedge-Shaped Region

The exact solutions presented so far have all been somewhat degenerate. In every case the form we assumed for the velocity profile caused the nonlinear inertia terms in the Navier-Stokes equation either to vanish completely or to produce only a centrifugal force, easily balanced by a pressure gradient. Since the mechanism of non-linear momentum transfer is best studied through exact solutions in which the non-linear terms play an important role, it is worthwhile to seek out such solutions.

In Fig. 4.7 consider that an incompressible fluid is contained in the trough between two non-parallel walls. Consider further that a line-source (or sink) of uniform output Q per unit length lies along the line of intersection of the walls. Let a

Fig. 4.7 Wedge geometry

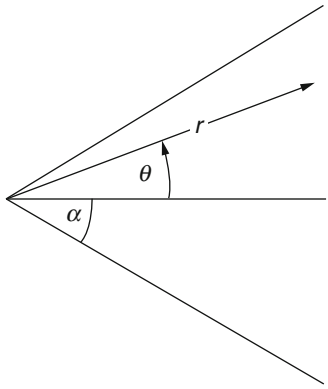

cylindrical polar coordinate system r, θ, z be defined so that the walls correspond to $\theta = \pm\alpha$. The velocity components must, then, satisfy the no-slip condition

$$v_r = v_\theta = v_z = 0 \quad \text{at } \theta = \pm\alpha, \tag{4.130}$$

along with the volume flow condition

$$\int_{-\alpha}^{\alpha} r v_r \, d\theta = Q \, . \tag{4.131}$$

We expect a priori that the flow will be two-dimensional. Moreover we suspect that a purely radial pattern of flow may satisfy the hydrodynamic equations. Therefore we seek a solution with

$$v_\theta = v_z = 0 \, . \tag{4.132}$$

The continuity equation (3.77) then requires that

$$v_r = \frac{1}{r} f(\theta) \, , \tag{4.133}$$

so that Eq. (3.79) becomes

$$\frac{\partial p}{\partial \theta} = \frac{2\mu}{r^2} f'(\theta) \, . \tag{4.134}$$

Thus

$$p = \frac{2\mu}{r^2} f(\theta) + g(r) \, . \tag{4.135}$$

Substituting (4.133) and (4.135) into (3.78) yields

$$r^3 g'(r) = \mu[f''(\theta) + 4f(\theta)] + \rho[f(\theta)]^2 \,. \tag{4.136}$$

Since the left side of (4.136) is a function of r alone and the right side is a function of θ alone, both sides must equal some constant, call it $-\mu K$. Then (4.135) yields

$$p = \frac{\mu}{2r^2}[4f(\theta) + K] + p_a \,, \tag{4.137}$$

where p_a is the pressure at $r = \infty$. Also (4.136) becomes a differential equation for $f(\theta)$:

$$f'' + 4f + \frac{f^2}{\nu} + K = 0 \,. \tag{4.138}$$

Integration of this equation introduces two new constants, which can be eliminated by use of the boundary conditions (4.130). The volume flow condition (4.131) then determines K.

Before proceeding, let us consider the consequences of the non-linear term in (4.138). Were it not for this term, the flow would be reversible: if f were a solution, then $-f$ would be a solution to the equation obtained by replacing K with $-K$, i.e., by replacing the source with a sink. However, with the non-linear term, which results from fluid inertia, no such conclusion can be drawn. Because of its inertia, the fluid attempts to obey Bernoulli's law, which relates the pressure to the fluid speed, not to the direction of flow; it is prevented from doing so by viscosity, which always acts to oppose the flow. If either inertia or viscosity were negligible, the flow would be reversible (in the first case $p - p_a$ would reverse sign; in the second case it would not). With both effects present, source flow differs qualitatively from sink flow. Discussions of the nature of the difference are presented in Goldstein (1938) and Schlichting (1960).

In order to obtain a first integral to (4.138), multiply through by f' and integrate. Since the geometry of Hamel's problem is symmetric with respect to the $\theta = 0$ axis, $f'(0) = 0$. Hence

$$\frac{1}{2}f'^2 + 2(f^2 - f_1^2) + \frac{1}{3\nu}(f^3 - f_1^3) + K(f - f_1) = 0 \,, \tag{4.139}$$

where f_1/r is the midstream velocity. Thus an implicit relation between f and θ can be obtained in terms of an elliptic integral:

$$\theta = \pm\sqrt{\frac{3\nu}{2}} \int_f^{f_1} \frac{df}{\sqrt{f_1 - f}\sqrt{f^2 + (f_1 + 6\nu)f + f_1^2 + 6\nu f_1 + 3\nu K}} \,. \tag{4.140}$$

Because of the symmetry about $\theta = 0$, either sign may be retained. If we choose the plus sign, the no-slip condition at $\theta = \alpha$ gives us

$$\int_0^{f_1} \frac{df}{\sqrt{f_1 - f}\sqrt{f^2 + (f_1 + 6\nu)f + f_1^2 + 6\nu f_1 + 3\nu K}} = \alpha\sqrt{\frac{2}{3\nu}} . \quad (4.141)$$

The second relation required to determine the constants f_1 and K is provided by the volume flow condition (4.131).

4.10.1 The Axisymmetric Analog of Hamel's Problem

Having succeeded in finding an exact solution to the problem of source flow in a wedge, we might try seeking another exact solution by considering flow from a source at the apex of a cone. As we shall see, the search leads quickly to a frustration.

Let a spherical coordinate system be chosen with origin at the apex of the cone and with $\theta = 0$ along its axis. Since the problem is axially symmetric, the orientation of the $\phi = 0$ axis is unimportant.

If we assume that, as in Hamel's problem, the flow pattern is purely radial, the continuity equation (3.101) requires that

$$v_r = \frac{1}{r^2} f(\theta) . \quad (4.142)$$

Equation (3.103) then becomes

$$\frac{\partial p}{\partial \theta} = \frac{2\mu}{r^3} f'(\theta) , \quad (4.143)$$

so that

$$p = \frac{2\mu}{r^3} f(\theta) + g(r) . \quad (4.144)$$

Substituting (4.142) and (4.144) into Eq. (3.102) yields

$$r^4 g'(r) - \frac{2\rho}{r}[f(\theta)]^2 = \mu[f''(\theta) + \cot\theta f'(\theta) + 6f(\theta)] . \quad (4.145)$$

Since the left side depends upon r and the right side does not, both sides must equal some constant, say C. But consider further: setting the left side of (4.145) equal to C yields

$$2\rho[f(\theta)]^2 = r^5 g'(r) - Cr . \quad (4.146)$$

Once more we find that both sides must equal some constant, so that $f(\theta)$ itself is constant. However, $f(\theta)$ vanishes at $\theta = \alpha$, where α is the semi-vertical angle of the cone. Consequently $f(\theta)$ is identically zero.

Thus we have shown that there can be no purely radial flow in a cone, at least for an incompressible fluid without body forces. There must be a component of flow in the θ-direction, so that an eddy pattern results. For such a pattern the Navier-Stokes equation is quite complicated. Hence there is not much hope for exact solution—especially as people have been trying ever since Georg Karl Wilhelm Hamel (1877–1954) published his paper in 1916 Hamel (1916).[2]

Some insight as to why radial flow obtains in a wedge but not in a cone comes from dimensional considerations. For wedge flow the relevant physical parameters are the fluid density, its viscosity, the wedge half-angle, and the source output per unit length. The dimensions of these quantities are

$$\begin{aligned} [\rho] &= ML^{-3} , \\ [\mu] &= ML^{-1}T^{-1} , \\ \alpha &: \text{ dimensionless} , \\ [Q] &= L^2T^{-1} . \end{aligned} \tag{4.147}$$

No combination of these parameters yields a length. If source flow in a wedge were to produce a steady-state eddy pattern, the eddies would presumably be characterized by a length, (for example, the distance from the origin beyond which no back-flow occurs,) expressible in terms of the parameters of the problem (for otherwise we would reach the ridiculous conclusion that it is a fundamental constant of the universe). As we have seen, however, the parameters do not give us such a length. For flow in a cone, however, the source strength, say Q^*, has dimensions of volume per unit time. Hence, $Q^*\rho/\mu$ is a length. Moreover, it depends on Q^* the way one might expect: as the source gets stronger, the eddies are blasted farther and farther out from the origin.

4.11 Bubble Dynamics

Let us now suppose that a spherical bubble of inviscid gas is contained in an otherwise unlimited volume of liquid. Suppose further that the pressure p_g of the gas forming the bubble varies with time. As a consequence the radius R of the bubble will also vary with time. The pulsating bubble will generate a velocity field within the liquid which in turn generates a stress field.

[2] A translation of the paper exists: United States NACA Technical Memorandum 1342. Since Hamel's result is extensively discussed in the hydrodynamics literature, his original paper is now primarily of historical interest.

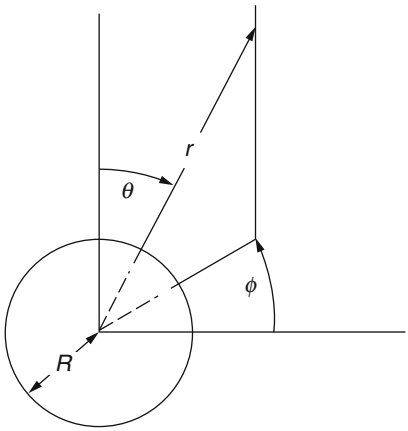

Fig. 4.8 Bubble geometry and spherical coordinates

The spherical symmetry of the situation makes it convenient to choose a spherical coordinate system with origin at the center of the bubble as in Fig. 4.8. The velocity field generated in the liquid will have only a radial component

$$v_r = v(r,t)\,, \tag{4.148}$$

so that the hydrodynamic equations (3.101) and (3.102) reduce to

$$\frac{\partial v}{\partial r} + \frac{2v}{r} = 0\,, \tag{4.149}$$

$$\rho\left[\frac{\partial v}{\partial t} + v\frac{\partial v}{\partial r}\right] = -\frac{\partial p}{\partial r} + \mu\left[\frac{\partial^2 v}{\partial r^2} + \frac{2}{r}\frac{\partial v}{\partial r} - \frac{2v}{r^2}\right]\,. \tag{4.150}$$

At the bubble wall, the liquid velocity must equal $\dot{R}(t)$, where an overdot denotes ordinary differentiation with respect to time. Thus integration of (4.149) yields

$$v = \frac{\dot{R}R^2}{r^2}\,. \tag{4.151}$$

Substituting this result into (4.150) and integrating, we obtain

$$\frac{(p-p_a)}{\rho} = \left(\frac{R}{r}\right)(R\ddot{R} + 2\dot{R}^2) - \left(\frac{R^4\dot{R}^2}{2r^4}\right)\,, \tag{4.152}$$

where p_a is the pressure at infinity.

With Eqs. (3.98) and (3.100), we see that the physical components of stress are given by

$$
\begin{aligned}
T_{rr} &= -p - \left(\frac{4\mu R^2 \dot{R}}{r^3}\right) , \\
T_{\theta\theta} &= T_{\phi\phi} = -p + \left(\frac{2\mu R^2 \dot{R}}{r^3}\right) , \\
T_{\theta\phi} &= T_{\phi r} = T_{r\theta} = 0 .
\end{aligned}
\tag{4.153}
$$

Within the bubble,

$$
\begin{aligned}
T_{rr} &= T_{\theta\theta} = T_{\phi\phi} = -p_g(t) , \\
T_{\theta\phi} &= T_{\phi r} = T_{r\theta} = 0 .
\end{aligned}
\tag{4.154}
$$

The stress components $T_{\phi r}$ and $T_{r\theta}$ must be continuous across the bubble surface. A comparison of (4.153) and (4.154) reveals that this requirement is automatically satisfied. The stress component T_{rr} must experience a jump of magnitude $2\tau/R$, where τ is the coefficient of interfacial tension ; the value inside the bubble is lower. Comparing the first of Eqs. (4.153) with the first of Eqs. (4.154), we find that the pressure just outside the bubble wall is given by

$$
p(R+0,t) = p_g(t) - \frac{(2\tau + 4\mu\dot{R})}{R} . \tag{4.155}
$$

By setting $r = (R + 0)$ in Eq. (4.152), we obtain an ordinary differential equation for the bubble radius as a function of time:

$$
R\ddot{R} + \frac{3}{2}\dot{R}^2 + \frac{4\mu\dot{R}}{\rho R} + \frac{2\tau}{\rho R} = \frac{p_g(t) - p_a}{\rho} . \tag{4.156}
$$

Since (4.156) is an equation of second order, two initial conditions must be specified. Most simply, $R(0)$ and $\dot{R}(0)$ will be given.

The treatment given here has been restricted to spherical bubbles. In practice, the presence of a unidirectional gravitational field tends to destroy the spherical symmetry. It also causes the bubble to rise in the liquid, and our analysis does not account for streaming past the bubble. Thus Eq. (4.156) is virtually useless in the study of large-scale bubbles arising, say, from an underwater explosion.

However in certain physical problems the bubble is small enough so that interfacial tension causes it to remain essentially spherical. When streaming past the bubble is negligible, Eq. (4.156) can then be applied. This approach has been used to study the growth of vapor bubbles in superheated liquids, Plesset and Zwick (1954), where the variation of p_g with time is caused by thermal expansion of the gas due to the diffusion of heat into the bubble. Also the growth of small bubbles by diffusion of gas through the liquid has been studied by use of Eq. (4.156), cf. Barlow and Langlois (1962) and Langlois (1963). Cavitation bubbles can also be

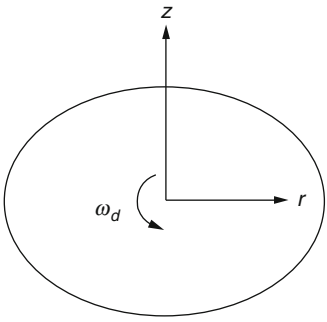

Fig. 4.9 Rotating disc

treated, but in the literature on cavitation in liquids, viscosity is usually neglected, so that the term $4\mu\dot{R}/\rho R$ is dropped from Eq. (4.156).

4.12 The Flow Generated by a Rotating Disc

As our next example of an exact solution to the equations of viscous hydrodynamics, we consider the flow generated by an infinite flat disc rotating in its own plane with constant angular velocity ω_d, as in Fig. 4.9. At first it would seem that purely rotary flow is generated, but, looking deeper, we see that this is not the case. First, solid body rotation is not an acceptable solution, for infinite pressures would be required to support the centrifugal forces generated by the rotating fluid. Therefore the fluid near the disc rotates faster than the fluid farther away. Consequently there is a variation of centrifugal force in the axial direction. The fluid near the disc is thrown outward more violently, so that other fluid must stream down the axis to replace it. Thus the motion is fully three-dimensional, albeit axisymmetric. By making a clever guess as to the form of the flow pattern, Theodore von Kármán (1891–1963) was able to reduce the hydrodynamic equations to a set of ordinary differential equations von Kármán (1921). He assumed that

$$v_r = ru(z), v_\theta = r\omega(z), v_z = v(z), p = p(z) . \tag{4.157}$$

Substituting these forms into Eqs. (3.77) through (3.80) yields

$$\begin{aligned} 2u + v' &= 0 , \\ u^2 - \omega^2 + u'v &= \nu u'' , \\ 2u\omega + \omega' v &= \nu\omega'' , \\ \rho v v' + p' &= \mu v'' . \end{aligned} \tag{4.158}$$

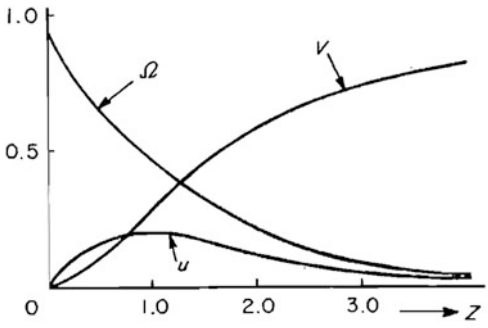

Fig. 4.10 Velocity components with respect to the normalized axial coordinate

These equations can be normalized by setting

$$z = \sqrt{\nu/\omega_d}\,Z, \quad u(z) = \omega_d U(Z), \quad \omega(z) = \omega_d \Omega(Z)\,.$$
$$v(z) = \sqrt{\nu\omega_d}\,V(Z), \quad p(z) = -\mu\omega_d P(Z)\,. \tag{4.159}$$

Thus

$$\begin{aligned} 2U + V' &= 0\,, \\ U^2 - \Omega^2 + U'V &= U''\,, \\ 2U\Omega + \Omega' V &= \Omega''\,, \\ VV' &= P' + V''\,. \end{aligned} \tag{4.160}$$

For boundary conditions, von Kármán assumed that the radial and azimuthal components of velocity approach zero as z approaches infinity. At $z = 0$, the no-slip condition applies. In terms of the normalized variables,

$$\begin{aligned} U = V = 0, \quad \Omega = 1 \quad &\text{at } Z = 0\,, \\ U \to 0, \Omega \to 0 \quad &\text{as } Z \to \infty\,. \end{aligned} \tag{4.161}$$

von Kármán obtained an approximate solution to the system (4.160) subject to the boundary conditions (4.161). We shall not go into the details, nor into those of Cochran's numerical solution Cochran (1934) for they are set out in Goldstein (1938) and Schlichting (1960)

As shown in Fig. 4.10, the significant point is that the radial and azimuthal velocity components differ appreciably from zero only in a layer near the disc. The thickness of this layer is proportional to $\sqrt{\nu/\omega_d}$ which therefore plays the role of a depth of penetration for the flow generated by a rotating disc. As $z \to \infty$, the axial component of velocity approaches asymptotically the finite value $-0.886\sqrt{\nu\omega_d}$ so that the rotating disc acts as a centrifugal pump.

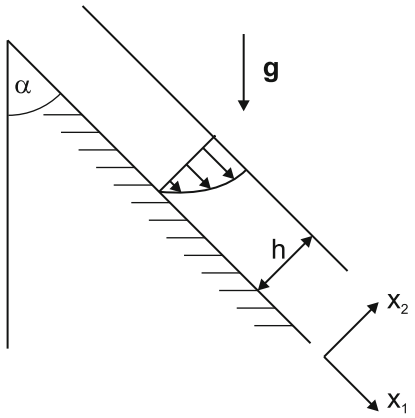

Fig. 4.11 Flow over an inclined plane

4.13 Free Surface Flow over an Inclined Plane

Taking the effect of gravity into account, consider the steady two-dimensional flow of a viscous fluid over a plane inclined with respect to the vertical direction by the angle α (cf. Fig. 4.11). The thickness of the fluid layer is uniform and equal to h. The fluid is in contact at the free surface with ambient air, which we will model as an inviscid fluid at pressure p_a. We assume that the air flow does not affect the viscous fluid flow. The flow is parallel as the trajectories of the fluid particles are parallel to the inclined plane. Therefore $\mathbf{v} = (v_1, 0, 0)$. By the incompressibility constraint, one obtains

$$\frac{\partial v_1}{\partial x_1} = 0, \tag{4.162}$$

and we deduce $v_1 = v_1(x_2)$. The only non zero component of the stress tensor is T_{12} or T_{21}. As pressure is uniform at the free surface, the pressure in the viscous fluid does not depend on the x_1 direction, but does depend on x_2. The first equation of (2.95) written in the x_1 direction yields

$$\frac{\partial T_{12}}{\partial x_2} + \rho g_1 = \frac{\partial T_{12}}{\partial x_2} + \rho g \cos\alpha = 0\,. \tag{4.163}$$

Integration of this relation yields

$$T_{12} = -\rho g\, x_2 \cos\alpha + C\,. \tag{4.164}$$

At the free surface $x_2 = h$, the shear stress must vanish as the inviscid fluid cannot sustain shear. One obtains

$$T_{12} = \rho g \cos\alpha (h - x_2)\,. \tag{4.165}$$

As $T_{12} = \mu\, dv_1/dx_2$, we may evaluate v_1 by integrating Eq. (4.165) with respect to x_2, with the boundary condition $v_1(x_2 = 0) = 0$. The velocity profile is given by

$$v_1 = \frac{\rho g \cos\alpha}{2\mu} x_2(2h - x_2)\ . \tag{4.166}$$

The Navier-Stokes equation in the x_2 direction gives the relation

$$-\frac{\partial p}{\partial x_2} + \rho g_2 = -\frac{\partial p}{\partial x_2} - \rho g \sin\alpha = 0\ . \tag{4.167}$$

Integrating with respect to x_2 and using the free surface condition $p(x_2 = h) = p_a$, we get

$$p = p_a - (\rho\, g \sin\alpha)(x_2 - h)\ . \tag{4.168}$$

The mass flux per unit length in the x_3 direction reads

$$Q = \int_0^h u\, dx_2 = \frac{\rho g \cos\alpha\, h^3}{2\mu}. \tag{4.169}$$

4.14 Natural Convection Between Two Differentially Heated Vertical Parallel Walls

We now consider the steady, two-dimensional, non-isothermal slow flow of a viscous incompressible fluid subjected to a variable temperature field. The fluid flows between two infinite vertical parallel walls at different temperatures, cf. Fig. 4.12, such that $\Theta_1 > \Theta_2$. We assume that the Boussinesq approximation is valid and the relevant equations are given by (2.196)–(2.198). The velocity field is a priori of the form $\mathbf{v} = (u(x_1, x_2), v(x_1, x_2), 0)$. However as the flow is invariant with respect to translation in the x_2 direction, one concludes that it depends only on the x_1 coordinate. With (2.196),

$$\frac{\partial u}{\partial x_1} = 0\ . \tag{4.170}$$

As $u = 0$ at the walls, $u = 0$ and $v = v(x_1)$. The temperature gradient is oriented in the horizontal direction, so that the temperature field is such that $\Theta = \Theta(x_1)$. Consequently Eq. (2.198) becomes

$$\frac{d^2\Theta}{dx_1^2} = 0\ . \tag{4.171}$$

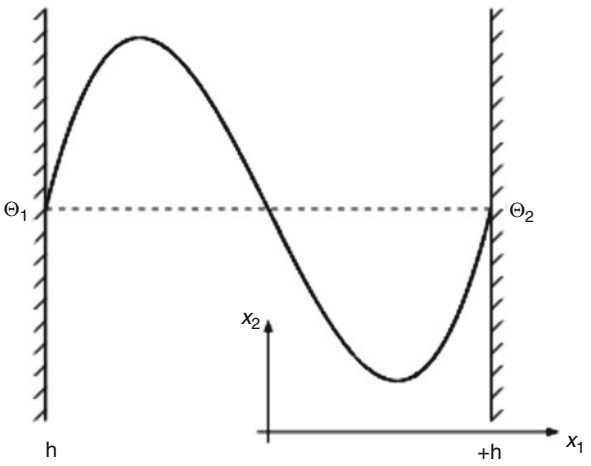

Fig. 4.12 Natural convection in an infinite plane channel

Integrating with the boundary conditions $\Theta = \Theta_1$ at $x_1 = -h$ and $\Theta = \Theta_2$ at $x = h$ yields

$$\Theta = \frac{\Theta_2 - \Theta_1}{2h} x_1 + \frac{\Theta_1 + \Theta_2}{2} = A x_1 + \frac{\Theta_1 + \Theta_2}{2} \,. \tag{4.172}$$

The momentum equation (2.197) gives

$$-\frac{\partial p}{\partial x_2} + \mu \frac{d^2 v}{dx_1^2} - \rho_0 g(1 - \alpha(\Theta - \Theta_0)) = 0 \tag{4.173}$$

The reference temperature is chosen such that $\Theta_0 = (\Theta_1 + \Theta_2)/2$, i.e. the mean temperature. As the flow is not driven by an exterior pressure gradient, the pressure is purely hydrostatic and results from the integration of

$$-\frac{\partial p}{\partial x_2} - \rho_0 g = 0 \,, \tag{4.174}$$

valid at equilibrium. Therefore the velocity field is driven by the buoyancy force and one solves

$$\mu \frac{d^2 v}{dx_1^2} + \rho_0 g \alpha A x_1 = 0 \,. \tag{4.175}$$

With the boundary conditions $v = 0$ at $x_1 = \pm h$,

$$v = \frac{g \alpha A}{6\nu} x_1 (h^2 - x_1^2) \,. \tag{4.176}$$

It is easy to verify that this velocity profile corresponds to a vanishing flow rate across each horizontal section. A posteriori the velocity field is orthogonal to the temperature field; this leads to the vanishing of the transport term in the material derivative of Θ.

In the real world, it is impossible to build infinite walls. Therefore top and bottom walls confine the fluid and force it to form a convection cell. The flow we have analyzed is thus unstable Koschmieder (1993) and constitutes an idealization of the physical phenomena.

4.15 Flow Behind a Grid

Kovasznay (1948) examines the steady state two-dimensional exact solution of the Navier-Stokes equation for the laminar flow behind a periodic array of cylinders or rods. The velocity field is assumed to be such that $v_1 = U + u_1, v_2 = u_2$, where U is the mean velocity in the x_1 direction. The vorticity equation (2.247) yields

$$\frac{\partial \xi_3}{\partial t} + (U + u_1)\frac{\partial \xi_3}{\partial x_1} + u_2 \frac{\partial \xi_3}{\partial x_2} = \nu \nabla^2 \xi_3 \,. \tag{4.177}$$

Denoting the spacing of the grid by δ, we define the Reynolds number as $\mathcal{R}e = \delta U/\nu$. The dimensionless vorticity becomes $\omega = \xi_3 \delta/U$. The other dimensionless variables are $x = x_1/\delta, y = x_2/\delta, \tau = tU/\delta, 1 + u = v_1/U, v = v_2/U$. The governing equation (4.177) is

$$\frac{\partial \omega}{\partial \tau} + (1 + u)\frac{\partial \omega}{\partial x} + v\frac{\partial \omega}{\partial y} = \frac{1}{\mathcal{R}e}\nabla^2 \omega \,. \tag{4.178}$$

As steady state solutions are sought, the term $\partial\omega/\partial\tau$ vanishes. We are left with

$$\nabla^2 \omega - \mathcal{R}e \frac{\partial \omega}{\partial x} - \mathcal{R}e \left(u\frac{\partial \omega}{\partial x} + v\frac{\partial \omega}{\partial y} \right) = 0 \,. \tag{4.179}$$

To build up the analytical solution, the trick consists in finding an expression that cancels the nonlinear term. The streamfunction is introduced to satisfy the continuity equation

$$u = \frac{\partial \psi}{\partial y}, \quad v = -\frac{\partial \psi}{\partial x} \,, \tag{4.180}$$

and therefore the vorticity is

$$\omega = -\nabla^2 \psi \,. \tag{4.181}$$

Taking the periodicity into account, the streamfunction is set up such that

$$\psi = f(x) \sin 2\pi y \ . \tag{4.182}$$

With (4.182), the nonlinear term of (4.179) gives

$$f' f'' - f f''' = 0 \ . \tag{4.183}$$

Integrating (4.183) we obtain

$$f'' = k^2 f \ , \tag{4.184}$$

where k is a real or complex arbitrary constant. A further integration yields

$$f = Ce^{kx} \ . \tag{4.185}$$

With the stream function

$$\psi = Ce^{kx} \sin 2\pi y \tag{4.186}$$

canceling the nonlinear term in (4.179), we have to seek a solution of the equation

$$\nabla^2 \omega - \mathcal{R}e \frac{\partial \omega}{\partial x} = 0 \ . \tag{4.187}$$

Setting

$$\omega = g(x) \sin 2\pi y \ , \tag{4.188}$$

we have

$$g'' - \mathcal{R}e \, g' - 4\pi^2 g = 0 \ , \tag{4.189}$$

the solution of which is

$$g(x) = Ae^{\lambda_1 x} + Be^{\lambda_2 x} \ , \tag{4.190}$$

where

$$\lambda_{1,2} = \frac{\mathcal{R}e}{2} \pm \sqrt{\frac{\mathcal{R}e}{2} + 4\pi^2} \ . \tag{4.191}$$

Combining (4.188) and (4.190), the vorticity is

$$\omega = \left(Ae^{\lambda_1 x} + Be^{\lambda_2 x}\right) \sin 2\pi y \ , \tag{4.192}$$

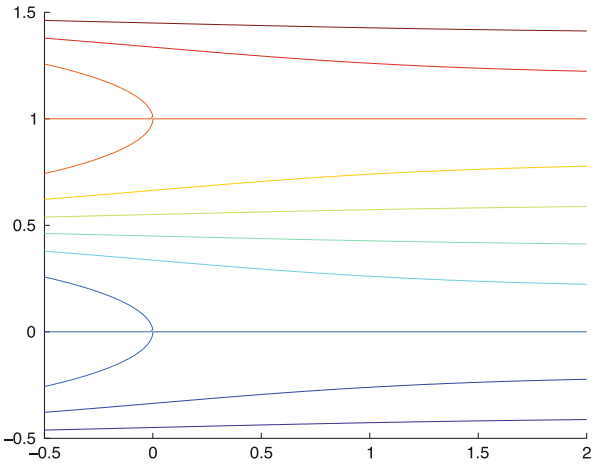

Fig. 4.13 Streamlines of the Kovasznay flow for $\mathcal{R}e = 40$

while Eqs. (4.181) and (4.186) give

$$\omega = C(4\pi^2 - k^2)e^{kx} \sin 2\pi y \ . \tag{4.193}$$

Comparison of (4.192) and (4.193) shows that two solutions are possible

$$k = \lambda_1, \quad A = -\mathcal{R}e\lambda_1 C, \quad B = 0, \tag{4.194}$$

$$k = \lambda_2, \quad A = 0, \quad B = -\mathcal{R}e\lambda_2 C, \tag{4.195}$$

With λ_2 and $\mathcal{R}e = 40$ the streamlines are shown in Fig. 4.13, with pairs of eddies generated behind the cylinders. The flow recovers uniformity downstream through the exponential term of the solution.

As the Kovasznay flow incorporates the nonlinear term, it is a good benchmark to test the numerical accuracy and space convergence of computational methods integrating the Navier-Stokes equation.

4.16 Plane Periodic Solutions

Many exact solutions of the Navier-Stokes equations are obtained for spatial periodic conditions. In this section we consider a two-dimensional (2D) solution due to Walsh (1992).

Let us first proof the following theorem

Theorem 4.1. *Let us consider a vector field* $\mathbf{u}$ *in the domain* Ω *that satisfies*

$$\nabla^2 \mathbf{u} = \lambda \, \mathbf{u}, \tag{4.196}$$

$$div \, \mathbf{u} = 0 \ . \tag{4.197}$$

Then the velocity $\mathbf{v} = e^{\nu\lambda t}\mathbf{u}$ *satisfies the Navier-Stokes equation (2.178) and (2.179) with a pressure such that*

$$\nabla p = -\mathbf{v} \cdot \nabla \mathbf{v} \,. \tag{4.198}$$

The vector $\mathbf{v}$ is divergence free as is also $\mathbf{u}$. Furthermore,

$$\frac{\partial \mathbf{v}}{\partial t} = \nu\lambda \mathbf{v} = \nu \Delta \mathbf{v} \,. \tag{4.199}$$

It remains to prove that the nonlinear term is a gradient. This amounts to showing that

$$\frac{\partial}{\partial x_2}\left(v_1 \frac{\partial v_1}{\partial x_1} + v_2 \frac{\partial v_1}{\partial x_2}\right) = \frac{\partial}{\partial x_1}\left(v_1 \frac{\partial v_2}{\partial x_1} + v_2 \frac{\partial v_2}{\partial x_2}\right) \,, \tag{4.200}$$

as $\mathbf{curl}\, \nabla = \mathbf{0}$. This is evident by incompressibility and relation (4.199).

In the 2D case, we resort to the streamfunction ψ, assuming that it is an eigenfunction of the Laplacian with eigenvalue λ. Consequently, $\mathbf{u} = (\partial\psi/\partial x_2, -\partial\psi/\partial x_1)$ satisfies (4.196) and (4.197)with the same λ. Therefore, $e^{\nu\lambda t}\psi$ is the streamfunction of the associated Navier-Stokes flow. If we have a periodic domain of size 2π, then the eigenfunctions λ are of the form $\lambda = -(k_{x_1}^2 + k_{x_2}^2)$, with k_{x_1} and k_{x_2} positive integers. For given k_{x_1}, k_{x_2}, the linearly independent eigenfunctions are

$$\cos(k_{x_1}x_1)\cos(k_{x_2}x_2), \sin(k_{x_1}x_1)\sin(k_{x_2}x_2) \,,$$
$$\cos(k_{x_1}x_1)\sin(k_{x_2}x_2), \sin(k_{x_1}x_1)\cos(k_{x_2}x_2) \,.$$

It is possible to build up complicated geometrical patterns by combination of the eigenfunctions named n, m eigenfunction by Walsh, with $\lambda = -(n^2 + m^2)$. A theorem in number theory shows that integers of the form p^{2i} and p^{2i+1}, where p is an integer number such that $p \equiv 1 \pmod 4$, may be written as sums of squares in exactly $i + 1$ manners. For example, $625 = 25^2 = 24^2 + 7^2 = 20^2 + 15^2$. Figure 4.14 displays the streamlines corresponding to $\psi = \sin(25x_1) + \cos(25x_2) - \sin(24x_1)\cos(7x_2) + \cos(15x_1)\cos(20x_2) - \cos(7x_1)\sin(24x_2)$.

4.17 Summary

The exact solutions presented in this chapter do not exhaust the list of those available, but they are fairly representative. A more comprehensive collection can be obtained by consulting the references.

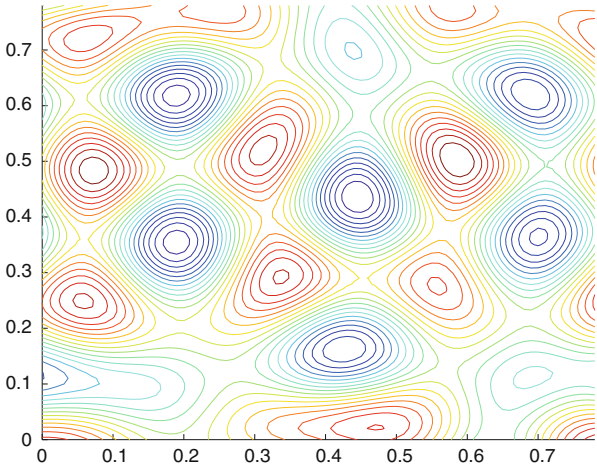

Fig. 4.14 ψ isocontours in the square $(0, \pi/4)^2$

Some flow problems such as the flow between parallel plates or in an annular region, are amenable to exact solution because the nonlinear inertia terms drop out of the hydrodynamic equations. Others, such as Hamel's problem, retain a nonlinear character, but enough nonlinear terms disappear so that the problem reduces to a differential equation whose solution can be recognized. Finally, there are flow problems, such as the flow generated by a rotating disc, which can be reduced to a system of normalized ordinary differential equations to be integrated numerically.

A semantical question arises: What is meant by "exact solution"? The answer probably varies from one era to another. In the mid-nineteenth century Hamel's solution probably would not have qualified, for it cannot be expressed in terms of functions well understood at that time. In the earlier twentieth century von Kármán's formulation of the rotating disc problem might not have been accepted as an exact solution because of the numerical labor that remained to be done.

Perhaps now we have come full cycle on von Kármán's problem: the student today might well ask if the numerical integration of four ordinary differential equations is any more an exact solution than would be numerical integration of the full hydrodynamic equations. However let us recall the state of computational art in the 1920s and 1930s. Numerical integration methods for both ordinary and partial differential equations were known, and the construction of analog computers was in sight. However high speed digital equipment, which makes practical the numerical treatment of partial differential equations, was still a generation away. Thus the reduction of a problem to ordinary differential equations really was a significant step.

Today much open source and commercial software is available. Visualization packages are also available to show the myriads of numerical results produced by simulation tools relying on high-performance computing. However the display of a result does not explain everything and simple (or simplified) models are still a source of understanding for what some people have named the incomprehensible Navier-Stokes equation.

http://www.springer.com/978-3-319-03834-6

Slow Viscous Flow

Langlois, W.E.; Deville, M.O.

2014, XV, 324 p. 133 illus., 7 illus. in color., Hardcover
ISBN: 978-3-319-03834-6